Chapter 4

MICROLYSIMETER PERFORMANCE

Recall that data presented in Chapter 3 showed that there was less evaporation from steel than from plastic microlysimeters (ML's) of 20 and 30 cm lengths. There also appeared to be a positive relationship between ML length and cumulative evaporation, at least for plastic ML's. Differences in thermal regime were evident with steel ML's warming and cooling more rapidly at depth than did plastic, i.e. heat flux was higher in steel ML's. Also temperature extremes were less for steel ML's which were cooler than plastic in daytime, confirming the findings of Salehi (1984), and warmer than plastic during the night. This chapter presents several statistical treatments of the data in order to clarify these relationships. Also presented are thermal diffusivity and heat flux calculations for the microlysimeter and field soil sites which were instrumented with thermistors to measure surface and subsurface temperatures.

<u>Evaporation.</u>

An analysis of covariance (ANCOVA) for total evaporation, mm, with the 2 wall types (plastic or steel) and the 2 blocks as the factors (main effects) and with length as a covariate showed that length had a significant effect on evaporation (5% level, Table 4-1, data from Table 3-1). The R^2 value was 0.70

and the overall model was significant at the 0.001% level. The effect of blocking was also highly significant, reinforcing the field observation that one block was wetter than the other.

The ANCOVA was performed using the GLM (General Linear Model) Procedure of the statistical program SAS on an IBM PC compatible computer. Procedure GLM can handle class variables (factors) having discrete levels (e.g. the walltype factor in Table 4-1 with plastic and steel as the 2 levels), and continuous variables (covariates) which measure quantities (e.g. the length covariate in Table 4-1) (SAS Institute Inc. 1985, p. 184). It can also handle unequal numbers of observations in the variables (SAS Institute Inc. 1985, p. 186). Since the ML data contained unequal numbers of observations and a covariate (length), Procedure GLM was chosen over a classical ANOVA procedure. The ANCOVA model is given in Appendix F and by the SAS Institute Inc. (1985, p. 210). A similar model is shown in detail by Neter and Wasserman (1974, p. 754).

A second ANCOVA, which was identical except that the first day's data were left out of the total, showed that neither wall type nor length were significant at the 10% level - a result which may not be surprising since at least a third of the total evaporation occurred on the first day after irrigation. The effects on evaporation of wall type or length

Table 4-1.

ANCOVA for total evaporation, E (mm), from microlysimeters with walltype and blocks as factors and length as a covariate.

SAS General Linear Models Procedure.
Class Level Information

Class	Levels	Values
BLOCK	2	0 1
WALLTYPE	2	0 1

Number of observations in data set = 17

Dependent Variable: E_MM

Source	DF	Sum of Squares	Mean Square	F Value	Pr > F
Model	3	38.2480	12.7494	10.13	0.0010
Error	13	16.3591	1.2584		
Corrected Total	16	54.6072			

R^2	C.V.	Root MSE	E_MM Mean
0.700422	9.4618	1.1218	11.86

Source	DF	Type III SS	Mean Square	F Value	Pr > F
BLOCK	1	25.6988	25.6988	20.42	0.0006
WALLTYPE	1	1.4405	1.4405	1.14	0.3041
LENGTH	1	5.7584	5.7584	4.58	0.0520

or both may be most important when the evaporation rate and soil water content are highest.

A repeated measures multiple analysis of covariance (MANCOVA) (SAS Institute Inc. 1985. p. 254) was performed using the daily evaporation data from Table 3-1 with wall type and blocks as factors and length as a covariate, and with 9 levels of time associated with the 9 days for which the dependent variable (daily evaporation) was measured. The effects of both length and blocks were significant at the 5 % level (Table 4-2). Walltype had no significant effect at the 10 % level. The hypothesis of no time effect was rejected at the 0.0001 % level, but interactions between time and walltype, time and blocks, and time and length were not significant at the 10 % level.

Omitting the biased data collected on the first day after irrigation, t-tests were done on the cumulative evaporation (mm) from the second through last day (9 days), comparing steel with plastic microlysimeters for each length (Table 4-3). There were no significant differences (10 % level) between plastic and steel ML's at any length but the fact that all steel ML's were 0.6 cm longer than plastic ones may have obscured differences. For the nominal 10 cm length, the 11.1 cm length of steel ML's was 6 % more than the 10.5 cm length of plastic ML's while evaporation from steel ML's was only 3 % more than that from plastic. Thus the discrepancy in length masked the fact that water loss from steel was actually less, on a volume basis, than that from plastic ML's at 10 cm nominal length.

Table 4-2.

Repeated measures ANCOVA for daily ML evaporation.

SAS General Linear Models Procedure, Class Level Information:

Class	Levels	Values
BLOCK	2	0 1
WALL	2	0 1

Number of observations in data set = 17

Repeated Measures Level Information:

Dependent Variable	E1	E2	E3	E4	E5	E6	E7	E8	E9
Level of TIME	1	2	3	4	5	6	7	8	9

MANOVA Test Criteria and Exact F Statistics for the Hypothesis of no TIME Effect:

Statistic	Value	F	Num DF	Den DF	Pr > F
Wilks' Lambda	0.01674	44.04	8	6	0.0001

MANOVA Test Criteria and Exact F Statistics for the Hypothesis of no TIME*BLOCK Effect:

Statistic	Value	F	Num DF	Den DF	Pr > F
Wilks' Lambda	0.2032	2.94	8	6	0.1029

MANOVA Test Criteria and Exact F Statistics for the Hypothesis of no TIME*WALL Effect:

Statistic	Value	F	Num DF	Den DF	Pr > F
Wilks' Lambda	0.3390	1.46	8	6	0.3309

MANOVA Test Criteria and Exact F Statistics for the Hypothesis of no TIME*LENGTH Effect:

Statistic	Value	F	Num DF	Den DF	Pr > F
Wilks' Lambda	0.2724	2.00	8	6	0.2063

Tests of Hypotheses for Between Subjects Effects:

Source	DF	Type III SS	Mean Square	F Value	Pr > F
BLOCK	1	2.8348	2.8348	20.24	0.0006
WALL	1	0.1771	0.1771	1.26	0.2812
LENGTH	1	0.7011	0.7011	5.00	0.0434
Error	13	1.8211	0.1401		

A t test, on the change in volumetric water content over the same period, showed no significant (10 % level) differences between steel and plastic ML's at either 10 or 30 cm lengths (Table 4-4).

Table 4-3.

T tests* on cumulative evaporation (mm) from day 93 - 101, comparing steel with plastic ML's at each of 10, 20 and 30 cm lengths.

Treatment	Mean Evap.	Variance	No. of samples			
Steel 10 cm.	8.070	0.02697	3	H: $\mu_S - \mu_P = 0$		
				t'	t(10 %)	Sign.
Plastic 10 cm.	7.859	0.03674	2	1.331	2.353	ns
Steel 20 cm.	7.780	0.00674	3	H: $\mu_S - \mu_P = 0$		
				t'	t(10 %)	Sign.
Plastic 20 cm.	8.578	0.64997	4	-1.668	1.895	ns
Steel 30 cm.	8.360	0.75839	2	H: $\mu_S - \mu_P = 0$		
				t'	t(10 %)	Sign.
Plastic 30 cm.	8.722	0.08268	2	-0.558	2.920	ns

* The test is a pooled t test for which the variances are assumed equal and the test statistic, t', is:

$$t' = (\mu_1 - \mu_2)/(S_p(1/n_1 + 1/n_2)^{1/2})$$

where v_1 and v_2 are the variances, μ_1 and μ_2 are the mean evaporation from steel and plastic ML's, and n_1 and n_2 are the number of samples. The pooled standard deviation, S_p, is given by:

$$S_p = [((n_1 - 1)v1 + (n_2 - 1)v2)/(n_1 + n_2 -2)]^{1/2}$$

and the degrees of freedom are (Montgomery 1976, p. 24):

$$DF = n_1 + n_2 - 2$$

There was a significant difference (10 % level), between 20 cm steel and plastic ML's, in the change in volumetric water content. With only two samples for each treatment at 30 cm length, the lack of significant differences between steel and plastic, in either cumulative evaporation or water content change, may not be especially meaningful. The experiment was designed to have three replicates at the 30 cm length but one of these was weighed only on the first and last days since thermistors were installed in the corresponding ML's. Since the first day's data were excluded from the t-test the replicate with thermistors installed was lost to the analysis. In fact, cumulative evaporation and change in water content were 4% and 6 % less, respectively, in 30 cm steel ML's compared to plastic.

Since the mid-day soil surface temperature depression, ($T_{o,max}$ - $T_{d,max}$), is theoretically related to daily evaporation and since ($T_{o,max}$ - $T_{d,max}$) was measured much more precisely than mass loss, an ANCOVA with ($T_{o,max}$ - $T_{d,max}$) as the dependent variable was performed with wall type and blocks as factors and length as a covariate. Excluding data from the first day after irrigation, it was found that both wall type and length affected ($T_{o,max}$ - $T_{d,max}$) significantly (10% level, r^2=0.13). This model was highly significant (Table 4-5). Because of the

Table 4-4.

T-tests* on average change in water content (m^3/m^3) from day 93 to day 101 comparing steel with plastic ML's at each of 10, 20 and 30 cm lengths.

Wall Material Length	Change in Water Content:					
Steel	Average	0.0727				
10 cm.	S.D.	0.00148				
	Variance	2.189E-06				
Plastic	Average	0.0748				
10 cm.	S.D.	0.00183	t'	DF	$t_{10\%}$	sign.
	Variance	3.332E-06	-1.46	3	2.35	no
Steel	Average	0.0369				
20 cm.	S.D.	0.00039				
	Variance	1.514E-07				
Plastic	Average	0.0419				
20 cm.	S.D.	0.00393	t'	DF	$t_{10\%}$	sign.
	Variance	1.547E-05	-2.13	5	1.90	yes
Steel	Average	0.0269				
30 cm.	S.D.	0.0028				
	Variance	7.841E-06				
Plastic	Average	0.0286				
30 cm.	S.D.	0.0009	t'	DF	$t_{10\%}$	sign.
	Variance	8.888E-07	-0.82	2	2.92	no

* The test is a pooled t test for which the variances are assumed equal and the test statistic, t', is:

$$t' = (\mu_1 - \mu_2)/(S_p(1/n_1 + 1/n_2)^{1/2})$$

where v_1 and v_2 are the variances, μ_1 and μ_2 are the mean changes in water content in steel and plastic ML's, and n_1 and n_2 are the number of samples. The pooled standard deviation, S_p, is given by:

$$S_p = [((n_1 - 1)v1 + (n_2 - 1)v2)/(n_1 + n_2 -2)]^{1/2}$$

and the degrees of freedom are (Montgomery 1976, p. 24):

$$DF = n_1 + n_2 - 2$$

strong correlation between daily evaporation and ($T_{o,max}$ - $T_{d,max}$) (shown in Chapter 6), one might initially conclude that these ANCOVA results imply a difference in evaporation between steel and plastic ML's. Later in this chapter it will be shown that differences in heat flux between the two wall types are important enough to account for the effect of wall type on ($T_{o,max}$ - $T_{d,max}$) independently of any difference in evaporation.

Table 4-5.

ANOVA for midday (T_o - T_d) with length as a covariate and wall type as a factor. Data from first day after irrigation eliminated.

Source of variation	Sum of Squares	DF	Mean Square	F	Significance of F
Covariates:					
Length	22.831	1	22.831	3.11	.080
Main effects:					
Walltype	89.314	1	89.314	12.15	.001
Block	33.333	1	33.333	4.54	.035
Explained	145.478	3	48.493	6.60	.000
Residual	970.179	132	7.350		
Total	1115.657	135	8.264		

The correlation coefficient was 0.130.

Linear regression analysis of total evaporation, mm, at experiment's end, with length as the independent variable, showed that the slope (0.10) was significantly different from zero (10% level, r^2 = 0.18). Regression analysis using dummy variables for wall type revealed no significant differences in the intercepts and slopes of regression lines established for plastic and steel ML's.

Regression analysis with dummy variables for wall type was analogous to the ANCOVA performed earlier but without blocking. Its purpose was to establish separate regression lines for steel and plastic ML's within a single regression analysis. The advantages of this are at least two fold. First, the error degrees of freedom (D.F.) are reduced by only one with the inclusion of the dummy variable whereas separation of the data into two separate analyses would cut the D.F. about in half, greatly reducing the power of any statistical tests. Secondly, many statistical analysis programs will output a covariance table for the regression coefficients which allows easy testing of differences between the slopes established for different treatments, e.g. a test of difference between the plastic and steel wall types becomes a test for significant difference in the line slopes. See Appendix E for more discussion on the use of dummy variables.

Analysis of the residuals (from the regression analysis with dummy variables) showed a distinct trend in the data (Figure 4-1). ML's that were weighed early on the day after irrigation (day 92) showed positive residuals and those weighed late in the day showed negative residuals. For the first few ML's weighed on day 92, from 30 to 40% of the total evaporation measured occurred during that first day after irrigation; but, for the last few ML's weighed that day, only 10 to 20% of the total evaporation occurred on that day. Considerable evaporation occurred during the several hours that separated the weighing of the first and last ML's, see Figure 3-1. This systematic error affected all the results even though the blocking in the experimental design and the order of weighing should have eliminated some of the bias by ensuring that treatments were interspersed in an ordered way during measurement (Table 3-1).

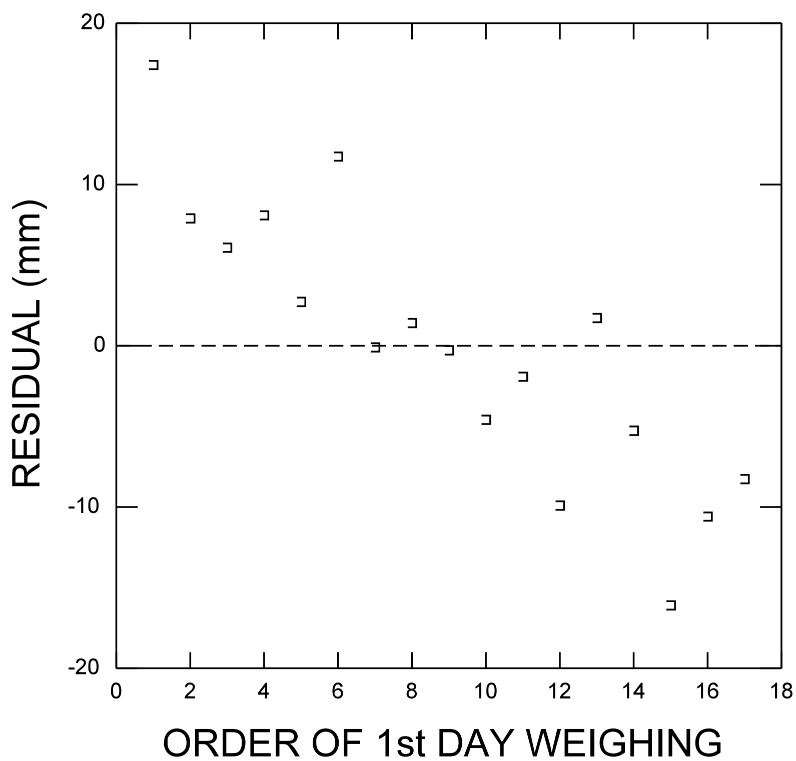

Figure 4-1. Residuals from regression of total ML evaporation vs. ML length with a dummy variable for walltype.

Since in theory the mid-day soil surface temperature depression, ($T_{o,max}$ - $T_{d,max}$), is closely related to daily evaporation, regressions were performed for actual daily evaporation E_a, mm, with ($T_{o,max}$ - $T_{d,max}$) as the independent variable and several combinations of dummy variables representing the treatments to show the effects, if any, of length and wall type.

Linear regression analysis with daily evaporation, mm, as the dependent variable and the quantity ($T_{o,max}$ - $T_{d,max}$) as the independent variable showed that the slope was highly significant (0.01% level, Table 4-6) but that the intercept was insignificant (10% level, r^2=0.50). The correlation coefficient at 0.50 was somewhat lower than the coefficient of 0.61 found by Ben-Asher et. al. (1983) for a similar regression analysis. There was considerable scatter in the data and residual analysis showed a definite trend but only in the first day's data. As in the residual analysis mentioned above, those ML's weighed early on the first day gave positive residuals and those ML's weighed later gave negative residuals. Ten of the 17 residuals were more than 1 standard deviation from the estimate of mean evaporation.

Further regression analysis of ($T_{o,max}$ - $T_{d,max}$) against E_a used dummy variables for the treatments following the model

Table 4-6.

Regression analyses for daily evaporation E_a (mm) with the midday soil surface temperature depression ($T_{o,max}$ - $T_{d,max}$) (°C), as the independent variable; and dummy variables for length and wall type treatments. All days included.

Model: $E_{est} = b_0 + b_1(T_{o,max} - T_{d,max})$

r^2 = 0.501, n = 153.

parameter	estimate	std. error	significance
intercept	0.075	0.130	0.566
($T_{o,max}$-$T_{d,max}$)	0.137	0.011	0.0001

Model: $E_a = b_0 + b_1x_1 + b_2x_2 + b_3x_3 + b_4x_4 + b_5x_5 + b_6E_{est}$

$$+ b_{16}x_{16} + b_{26}x_{26} + b_{36}x_{36} + b_{46}x_{46} + b_{56}x_{56}$$

See Appendix E for explanation of model.

r^2 = 0.568

parameter	estimate	std. error	significance
intercept	0.285	0.356	0.42
x_1	-0.397	0.483	0.41
x_2	0.288	0.442	0.52
x_3	-0.699	0.478	0.15
x_4	0.049	0.435	0.91
x_5	-1.249	0.548	0.02
($T_{o,max}$ - $T_{d,max}$)	0.123	0.030	0.00
x_{16}	0.017	0.041	0.68
x_{26}	-0.047	0.039	0.23
x_{36}	0.046	0.040	0.25
x_{46}	0.002	0.037	0.96
x_{56}	0.118	0.044	0.01

Equations:

E_a = -0.112 + 0.141 ($T_{o,max}$ - $T_{d,max}$), 10 cm, steel
E_a = 0.573 + 0.170 ($T_{o,max}$ - $T_{d,max}$), 10 cm, plastic
E_a = -0.414 + 0.169 ($T_{o,max}$ - $T_{d,max}$), 20 cm, steel
E_a = 0.334 + 0.125 ($T_{o,max}$ - $T_{d,max}$), 20 cm, plastic
E_a = -0.964 + 0.241 ($T_{o,max}$ - $T_{d,max}$), 30 cm, steel
E_a = 0.285 + 0.123 ($T_{o,max}$ - $T_{d,max}$), 30 cm, plastic

presented in Appendix E. Six regression lines resulted, 3 lines for plastic ML's and 3 lines for steel ML's (Table 4-6, Figure 4-2). The correlation coefficient of 0.57 was fairly close to the figure of 0.61 obtained by Ben-Asher et al. (1983). The intercept terms were insignificant at the 10% level except for the intercept term associated with 30 cm long steel microlysimeters which at -0.96 was the most negative intercept. The slope term associated with the quantity ($T_{o,max}$ - $T_{d,max}$) was highly significant (0.0001% level) as was the slope for the 30 cm long steel ML's (0.01% level) which at 0.241 was the highest slope and almost twice the mean slope of 0.137. All other slope terms were not significant at the 10% level. Line slopes for 20 and 30 cm plastic ML's were lower than those for steel and intercepts for plastic ML's were all positive while those for steel ML's were all negative. The slopes for 20 and 30 cm long plastic ML's were significantly lower than those for 20 and 30 cm long steel ML's (10% level).

Plotting of the residuals again showed a trend for first day values that was associated with the time of initial weighing. Microlysimeters weighed early on the first day showed positive residuals, including 2 residuals more than 2 SD from the mean estimate, and those ML's weighed late on the first day again showed negative residuals, including 2 residuals more than 2 SD from the mean estimate. A residual trend was observed for the last two days, with all but 3

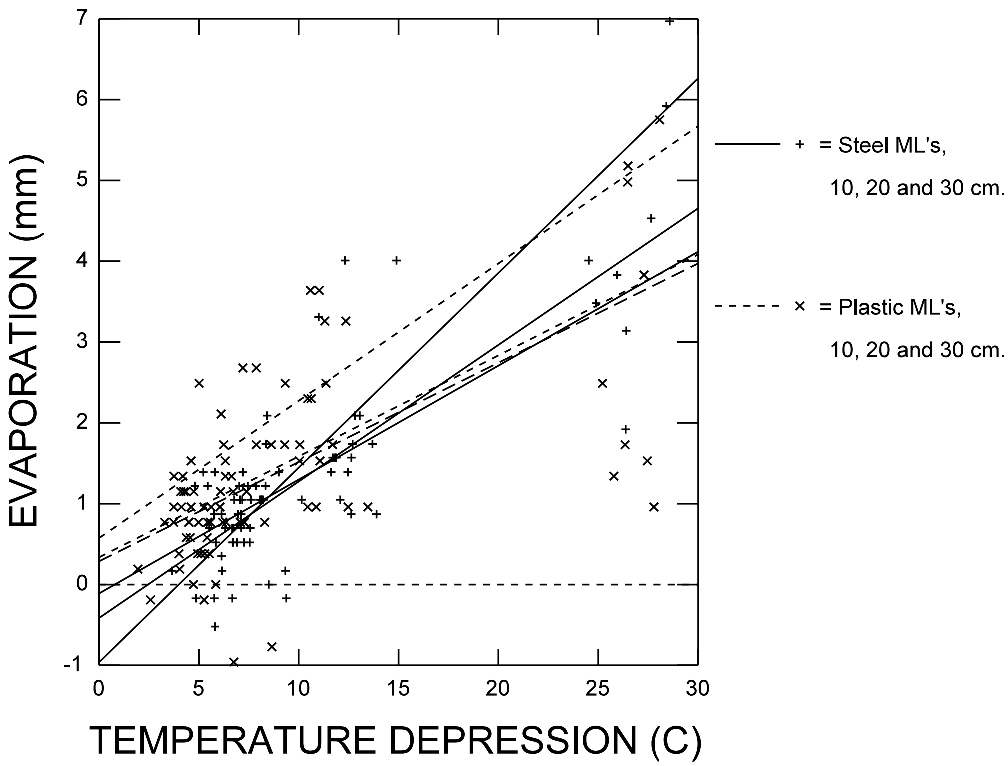

Figure 4-2. Linear regression of daily evaporation (mm) vs. ($T_{o,max}$ - $T_{d,max}$). Regression lines are for the six ML treatments. Higher position of the right end of each line equates to longer ML length.

residuals for day 8 being positive and all but one of the residuals for day 9 being negative. All of these latter residuals were less than 1 SD from the estimate and the trends were probably due to average wind speed being quite different on the 2 days.

Drainage.

Final ML water contents (g/g) were compared with water contents of adjacent field soil obtained by sampling with a King tube to depths of 10, 20 and 30 cm at the experiment's end. Except for 10 cm long plastic ML's, all length and walltype treatments were significantly wetter than the adjacent field soil (Pooled t tests on mean water contents, Table 4-7). For 30 cm plastic ML's the mean difference was 0.011 g/g which was equivalent to about 4.6 mm depth of water (assuming bulk density of 1.35 Mg m^{-3} in the top 30 cm of soil). A water depth of 4.6 mm represents 37 % of mean cumulative evaporation for 30 cm plastic ML's. An important question is what part of the 4.6 mm was lost to evaporation and what was lost to drainage? Although no data were gathered to answer this question, one might quess that there was more drainage and less evaporation from field soil than from the ML's.

Table 4-7.

Final water contents (g/g) in ML's compared to water contents of adjacent field soil sampled with a King tube.

Microlysimeters:

	S-10*	P-10	S-20	P-20	S-30	P-30
	0.121	0.108	0.156	0.156	0.175	0.184
	0.131	0.111	0.151	0.151	0.143	0.147
	0.112		0.142	0.151	0.162	0.165
				0.151	0.162	0.158
Average	0.1212	0.1098	0.1498	0.1525	0.1607	0.1636
Variance	5.99E-05	2.04E-06	3.41E-05	5.00E-06	1.27E-04	1.82E-04
N	3	2	3	4	4	4

King tube:

	10 cm	20 cm	30 cm
Average	0.106	0.138	0.152
Variance	1.58E-05	2.46E-05	4.91E-05
N	10	11	16

Pooled t tests**:

t'	DF	t(10 %)	Significance
Compare S-10 to 10 cm King tube:			
4.77	11	1.796	**
Compare P-10 to 10 cm King tube:			
1.355	10	1.813	ns
Compare S-20 to 20 cm King tube:			
3.465	12	1.782	**
Compare P-20 to 20 cm King tube:			
5.473	13	1.771	***
Compare S-30 to 30 cm King tube:			
1.910	18	1.734	*
Compare P-30 to 30 cm King tube:			
2.389	18	1.734	*

* Code: S = steel; P = plastic;
10, 20 and 30 = 10, 20 and 30 cm.

** The test is a pooled t test for which the variances are assumed equal and the test statistic, t', is:

$$t' = (\mu_1 - \mu_2)/(S_p(1/n_1 + 1/n_2)^{1/2})$$

where v_1 and v_2 are the variances, μ_1 and μ_2 are the means, and n_1 and n_2 are the number of samples. The pooled standard deviation, S_p, is given by:

$$S_p = [((n_1 - 1)v1 + (n_2 - 1)v2)/(n_1 + n_2 - 2)]^{1/2}$$

and the degrees of freedom are (Montgomery 1976, p. 24):

$$DF = n_1 + n_2 - 2$$

Soil Temperature and Heat Flux.

If there is no net soil warming or cooling, then the diurnal net soil heat flux is zero, a priori. In an irrigated field it is unlikely that such a condition would occur since the addition of large amounts of water can greatly change both soil temperature and heat capacity.

Diurnal deviations from the annual temperature cycle may be caused by assorted phenomena including cloudiness, regional air temperature changes, precipitation and irrigation. In the arid Southwest the largest sudden deviations, by far, would be caused by irrigation. For example, irrigation with 5 cm of water at 15 °C on a soil at 25 °C with an initial water content of 0.1 m^3/m^3 and a bulk density of 1.48 would immediately lower the temperature of the wetted layer to 20 °C (assuming negligible heat of wetting, the soil brought to saturation and a heat capacity of 1.54 MJ m^{-3} K^{-1}). Subsequent warming of the soil would be the result of net positive daily soil heat flux.

In the present study soil temperatures at 15 and 30 cm showed a strong linear warming trend of 6 to 7 °C over 7 days for all ML types and for the field soil (Figures 3-9 and 3-12) indicating substantial net positive heat flux. There were significant (<1% level) differences between steel and plastic ML's in the timing of subsurface temperature maxima and minima (Table 4-8) while at the surface there was no such difference

Table 4-8.

T tests on the phase shift in hours between the times of temperature maxima and minima in steel microlysimeters and those in plastic microlysimeters, at 15 and 30 cm depths.

	Daily maxima		Daily minima	
	15 cm	30 cm	15 cm	30 cm
Phase shift in temperature maxima and minima, hours.	1.41	3.03	1.25	2.81
Standard deviation of the difference, hours.	0.129	0.364	0.189	0.291
Value of the t statistic, 7 DF.	30.74	23.53	18.71	27.31
Significance level	<1.0%	<1.0%	<1.0%	<1.0%

showing that important differences existed in the gross conductivity of steel vs. plastic ML's. Also, the average differences in daily soil temperature maxima and minima were significant at better than the 1% level for all depths (Table 4-9). During the day steel ML's were cooler than plastic at the surface but warmer below the surface. At night the surface temperature of steel ML's was significantly higher than that of plastic.

Clearly steel ML's conducted heat from and to the soil surface much more quickly than did plastic. Questions that arise then are: what is the value of soil heat flux in the ML's, how does this compare to heat flux in the undisturbed

Table 4-9.

T tests on the differences between plastic and steel microlysimeters in daily soil temperature maxima and minima at 3 depths. Differences were calculated by subtracting temperature in steel ML from temperature in plastic ML.

DAILY MAXIMA	Surface	15 cm	30 cm
Average difference between temperature maxima, °C.	1.486	-0.707	-0.540
Standard deviation of the difference, °C.	0.310	0.073	0.100
Value of the t statistic, 7 DF.	13.54	27.25	15.34
Significance level	<1.0%	<1.0%	<1.0%
DAILY MINIMA	**Surface**	**15 cm**	**30 cm**
Average difference between temperature minima, °C.	-1.201	0.297	0.249
Standard deviation of the difference, °C.	0.253	0.055	0.121
Value of the t statistic, 7 DF.	13.42	15.38	5.81
Significance level	<1.0%	<1.0%	<1.0%

field soil, and what effect would the heat flux have on the evaporation estimated from weighing the ML's.

The diffusion equation for heat conduction in one dimension is:

$$C_v \frac{\partial T}{\partial t} = k \frac{\partial}{\partial x} \left[\frac{\partial T}{\partial x} \right] \quad [4\text{-}1]$$

where C is the volumetric heat capacity [J m^{-3} K^{-1}], k is the thermal conductivity [J d^{-1} cm^{-1} K^{-1}], both assumed constant in space. Distance is denoted by x and temperature by T. The soil heat flux, G, is:

$$G = -k\ \partial T/\partial x \quad [4\text{-}2]$$

This is Fourier's law of heat conduction for constant conductivity.

Calculation of heat flux into the drying soil required that values of the thermal conductivity, k, and volumetric heat capacity, C_v, be known on at least a daily, if not more frequent, basis. Since the two parameters are related by the equation

$$\alpha = k/C_v \quad [4\text{-}3]$$

where α is the thermal diffusivity, it suffices to know the diffusivity and heat capacity values. This is fortunate since k is difficult to measure while α can be deduced using a harmonic analysis. Soil volumetric heat capacity [J m^{-3} K^{-1}] is relatively easy to approximate by

$$C_v = 2010000\ \rho_b/2.65 + 4190000\ \Theta_v \qquad [4\text{-}4]$$

where ρ_b is the soil bulk density, the value 2.65 is an assumed particle density, Θ_v is the volumetric water content and organic matter content is negligible (deVries 1963 or Hillel 1982, Eq. 9.16).

In preparation for calculation of soil heat fluxes in drying soil, apparent thermal diffusivities were calculated on a daily basis for the field soil and each ML treatment using an iterative, least sum-of-squares method (Horton et al. 1983). Calculations proceeded in 2 steps. First, a solution to the second law of heat conduction was fit to measured surface temperatures using linear least squares regression. In the second, iterative, step the solution, with fitted coefficients and an assumed value of α, was used to estimate temperatures at either the 15 or 30 cm depth and the sum of squared error between estimated and measured temperatures at that depth was calculated. The value of α was changed for each iteration and the value of α resulting in the smallest sum of squared error was chosen as the apparent diffusivity. Calculations used averaged temperatures (2 replicates) at each of the 0.5, 15 and 30 cm depths at 15 minute intervals starting at midnight and proceeding for 23.75 hours (96 intervals). The temperatures at 0.5 cm were corrected to surface temperatures by scaling to infrared-based surface temperatures as previously described.

The solution to the heat conduction equation was:

$$T(x,t) = \overline{T} + \sum_{n=1}^{M} \{C_{0n} \exp(-x(nw/(2\alpha))^{1/2}) \sin(nwt + \phi_{0n} - x(nw/(2\alpha))^{1/2})\} \qquad [4-5]$$

with the frequency w given by $w = 2\pi/24$. For $x = 0$, Equation 4-5 reduces to:

$$T(0,t) = \overline{T} + \sum_{n=1}^{M} C_{0n} \sin(nwt + \phi_{0n}) \qquad [4-6]$$

which is the upper boundary condition for the solution. The lower boundary condition is:

$$T(\infty,t) = \overline{T} \qquad [4-7]$$

Equation 4-6 is equivalent to:

$$T(0,t) = \overline{T} + \sum_{n=1}^{M} [A_{0n} \sin(nwt) + B_{0n} \cos(nwt)] \qquad [4-8]$$

where $\phi_{0n} = \mathrm{Tan}^{-1}(B_{0n}/A_{0n})$ and $C_{0n} = A_{0n}/\sin(\phi_{0n})$. The coefficients in Equation 4-8 with $M = 6$ were easily found by multiple least squares linear regression. Most R^2 values were greater than 0.99. Using the fitted values of ϕ_{0n} and C_{0n}, Equation 4-5 was used to predict the temperature at either 15 or 30 cm depth while the value of diffusivity was changed iteratively until the sum of squared error (SSE), between predicted and actual temperatures at that depth, was minimized (program NR.BAS, Appendix C). The iterations were repeated several times, with progressively smaller changes between the values of diffusivity, until the value of apparent diffusivity associated with the minimum SSE was known to 4 significant digits.

Apparent diffusivities calculated using this method were markedly higher for steel than for plastic ML's (Figure 4-3, Table 4-10). This result was undoubtedly due to the much higher thermal conductivity of steel as compared to plastic. The thermal conductivity of carbon steel is more than three orders of magnitude larger than that of rigid polyvinyl chloride (PVC) (about 4 and 0.0015 J/(s cm °K), respectively, Touloukian et al. 1970). Also, the water contents of plastic and steel ML's were similar for all days (Table 3-2). For the surface to 15 cm layer, plastic ML's of both types (open and closed bottoms) yielded diffusivities equal to those for field soil indicating that the plastic wall material was not acting as a heat conductor compared to the soil. Although the thermal conductivity of soil varies widely with water content, bulk density and other properties, a median value is on the order of 0.01 J/(s cm °K) and for dry soils k can be as low as 0.001 J/(s cm °K) (de Vries 1975, especially Fig. 2.1). Clearly, PVC will act as an insulator in most field situations while steel acts as a conductor relative to the soil.

For the surface to 30 cm layer the plastic ML's with open bottoms exhibited diffusivities close to those of the field soil while plastic ML's with closed bottoms exhibited higher diffusivities reflecting an effect of the insulating value of the plastic disk that closed the ML bottom. This disk would block both heat flux and drainage below the ML's. Higher water contents would not necessarily result in higher diffusivities since both thermal conductivity and heat capacity increase with water content. Indeed, the diffusivity of the surface to 30 cm layer is quite constant over time, indicating that drying of the soil in this wetness range (0.28 to 0.23 m^3/m^3) had little effect on apparent diffusivity (Figure 4-3). Thus the increased diffusivity values, calculated for ML's with closed bottoms, reflected temperatures at 30 cm that were abnormally higher due to the insulating disk.

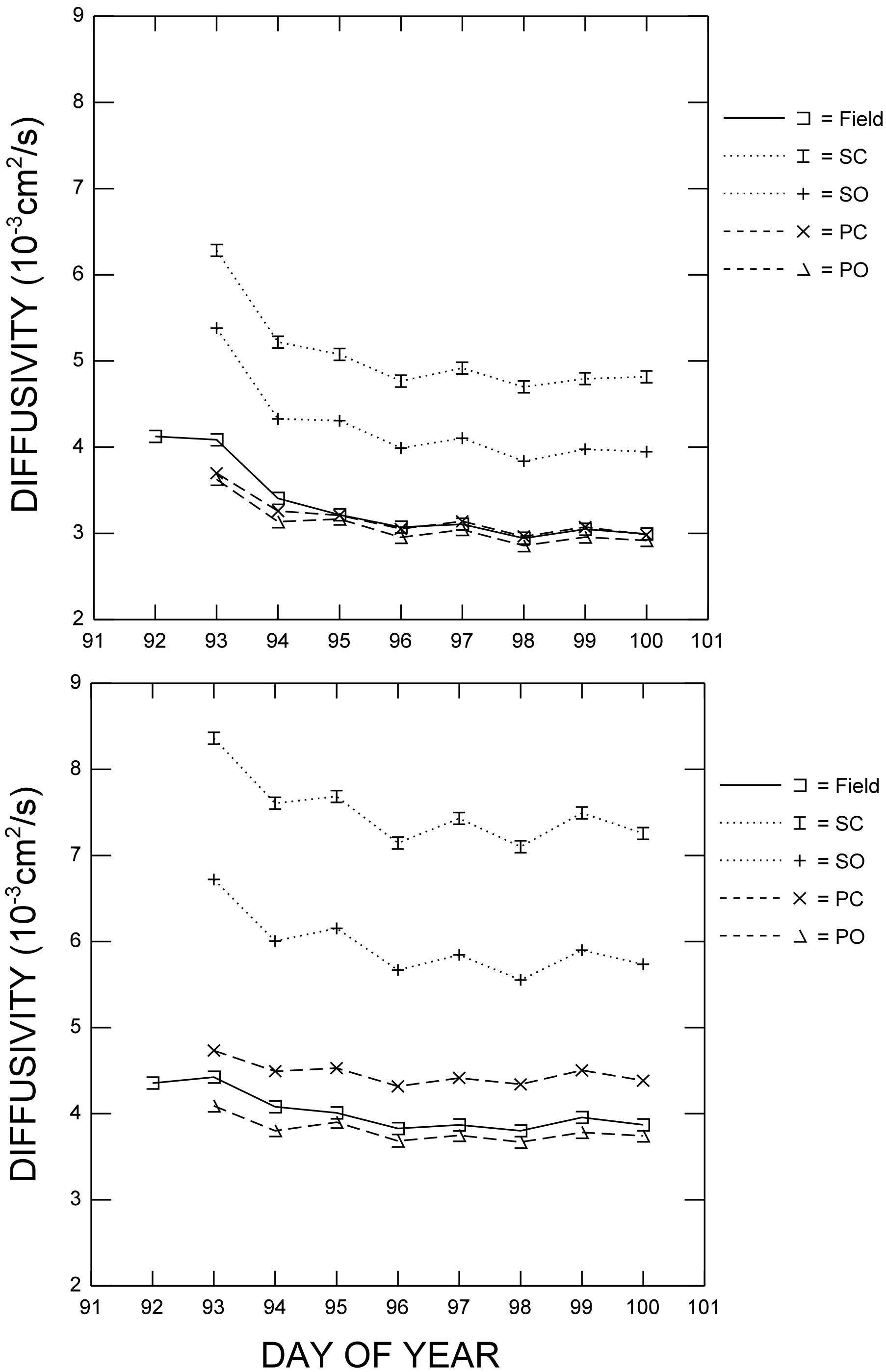

Figure 4-3. Thermal diffusivities calculated using harmonic analysis, for the 0 to 15 cm layer (top) and the 0 to 30 cm layer (bottom). S = steel, P = plastic, O = open, C = closed bottom.

Table 4-10.

Soil average temperature, ave. T [°C]; thermal diffusivity, α [10^{-3} cm^2/s]; and positive soil heat flux, G [mm of water equivalent]. (From harmonic analysis).

Code*		Day of Year 92	93	94	95	96	97	98	99	100	Averages
Fld 15, ave.	T	17.11	17.96	19.17	20.34	20.91	21.77	22.76	23.93	24.68	21.44
	α	4.13	4.09	3.41	3.22	3.07	3.11	2.94	3.05	3.00	3.23
	G	2.31	2.06	2.32	2.48	2.46	2.66	1.98	2.30	2.23	2.31
30, ave.	T	16.85	17.27	18.03	18.92	19.64	20.29	21.23	22.04	22.90	20.04
	α	4.36	4.43	4.08	4.01	3.83	3.87	3.80	3.96	3.87	3.98
	G	2.38	2.15	2.54	2.77	2.75	2.97	2.25	2.62	2.53	2.57
SC 15, ave.	T	-	18.44	19.46	20.66	21.30	22.33	23.30	24.54	25.30	21.92
	α	-	6.28	5.22	5.08	4.77	4.92	4.70	4.80	4.82	5.07
	G	-	2.46	2.68	2.85	2.93	3.09	2.36	2.73	2.62	2.72
30, ave.	T	-	17.73	18.48	19.42	20.15	20.97	21.99	22.95	23.82	20.69
	α	-	8.36	7.61	7.69	7.15	7.43	7.10	7.50	7.26	7.51
	G	-	2.84	3.23	3.51	3.58	3.80	2.90	3.41	3.22	3.31
SO 15, ave.	T	-	18.36	19.40	20.54	21.20	22.14	23.09	24.25	25.04	21.75
	α	-	5.38	4.33	4.31	3.99	4.11	3.84	3.98	3.95	4.24
	G	-	2.26	2.50	2.62	2.70	2.85	2.21	2.55	2.47	2.52
30, ave.	T	-	17.45	18.19	19.05	19.79	20.53	21.49	22.34	23.21	20.26
	α	-	6.72	6.01	6.15	5.67	5.85	5.55	5.90	5.74	5.95
	G	-	2.53	2.94	3.13	3.22	3.40	2.66	3.11	2.98	3.00
PC 15, ave.	T	-	18.34	19.27	20.43	21.13	22.06	23.05	24.20	25.03	21.69
	α	-	3.70	3.26	3.21	3.05	3.14	2.97	3.07	2.98	3.17
	G	-	2.11	2.35	2.61	2.63	2.80	2.06	2.47	2.35	2.42
30, ave.	T	-	17.62	18.26	19.09	19.87	20.59	21.60	22.41	23.33	20.35
	α	-	4.73	4.49	4.53	4.32	4.42	4.34	4.50	4.38	4.47
	G	-	2.39	2.76	3.10	3.12	3.32	2.49	2.99	2.84	2.88
PO 15, ave.	T	-	18.29	19.30	20.45	21.14	22.02	22.98	24.10	24.91	21.65
	α	-	3.63	3.14	3.17	2.95	3.04	2.86	2.96	2.92	3.08
	G	-	2.00	2.29	2.46	2.52	2.67	2.04	2.39	2.29	2.33
30, ave.	T	-	17.48	18.13	18.94	19.71	20.39	21.31	22.08	22.96	20.13
	α	-	4.09	3.80	3.90	3.68	3.75	3.67	3.78	3.74	3.80
	G	-	2.13	2.53	2.74	2.82	2.96	2.31	2.71	2.59	2.60

* Codes:
- Fld = field soil.
- SC = steel ML with closed bottom.
- SO = steel ML with open bottom.
- PC = plastic ML with closed bottom.
- PO = plastic ML with open bottom.
- 15 = surface to 15 cm layer.
- 30 = surface to 30 cm layer.

At this point it is well to reflect that the calculation method arises from one dimensional (1-D) heat transfer theory for a homogeneous soil while the steel ML walls and plastic disks represent severe to moderately severe departures from the 1-D theory. Also, as the soil dries the water content distribution becomes increasingly non-homogeneous. Still, the relative values of diffusivity are informative and the values should be fairly accurate for field soil and for plastic ML's without closed bottoms.

Taking the derivative of Equation 4-5 with respect to x, setting x = 0 and inserting the result in Equation 4-2 gives the heat flux at the soil surface:

$$G = \sum_{n=1}^{M} \{kC_{0n} \ (nw/\alpha)^{1/2} \sin[nwt + \phi_{0n} + \pi/4]\} \qquad [4\text{-}9]$$

Using the phase angle and amplitude coefficients found earlier for M = 6 and using the corresponding apparent diffusivities, the thermal conductivities were calculated using Equations 4-3 and 4-4 and apparent heat fluxes were calculated on a 15 minute interval for all ML types and for the field soil using Equation 4-9 (Appendix C). Summing only positive values for each day resulted in daily values of positive soil heat flux (Figure 4-4, Table 4-10). For both open and closed bottom types the apparent heat fluxes were clearly higher for steel ML's than for plastic ML's. Summing the heat fluxes over 24 hours resulted in the expected net heat flux of zero for the diurnal period. The zero value was pre-determined by the choice of Equation 4-7 as the lower boundary condition. That the actual net daily heat flux was certainly not zero for the present study may be inferred from the warming trends shown in Figure 3-11.

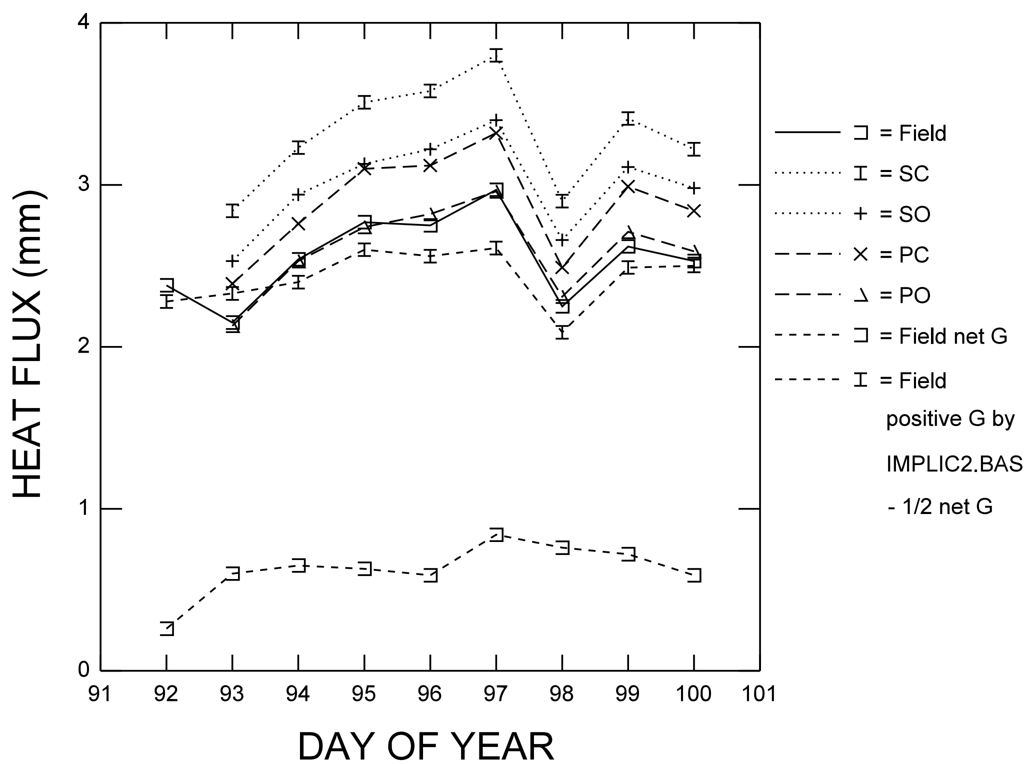

Figure 4-4. Positive and net daily soil heat flux. Field, SC, SO, PC and PO were calculated by harmonic analysis for the 0 to 30 cm layer. Net G and (G - 1/2 net G) were calculated by finite difference using the surface and 30 cm temperatures measured for field soil. S = steel, P = plastic, O = open and C = closed bottoms.

Since positive heat flux and evaporation occur in phase, the energy available for evaporation from steel ML's would be less than that available for evaporation from plastic ML's by the difference in positive heat flux between steel and plastic ML's. The average difference in positive flux between steel and plastic ML's with closed bottoms was 0.43 mm/d (Table 4-10). Over 9 days this difference might amount to a 3.9 mm difference in evaporation observed. The actual difference was 0.3 mm (Table 3-2). Equivalent calculations for 15 cm long ML's show that plastic might lose up to 2.7 mm more than do steel to evaporation over 9 days whereas the actual difference in cumulative evaporation was 0.8 mm. In reality the higher surface temperature of plastic compared to steel ML's would mean that plastic ML's would also lose more energy to sensible heat flux and long wave re-radiation to the sky. Therefore the calculations are not so simple.

In order to compute the net soil heat flux, a finite difference computer program was written (Appendix D) to solve the heat flow equation (4-1) subject to boundary conditions of known temperature:

$$T(0,t) = f_0(t) \qquad [4\text{-}10]$$

$$T(30,t) = f_{30}(t) \qquad [4\text{-}11]$$

where the functions $f_0(t)$ and $f_{30}(t)$ were represented discretely at 15 minute time intervals by the measured temperatures at the surface and 30 cm depth respectively. An analytical solution of [42] subject to [53] and [54] is given by Carslaw and Jaeger (1959, p. 102). The author found the finite difference solution easier to perform.

Using central differences for space, Equation 4-1 was represented as (Ozisik 1980, Equation 12-83):

$$-rT_{j-1}^{n+1} + (2 + 2r)T_j^{n+1} - rT_{j+1}^{n+1} = rT_{j-1}^{n} + (2 - 2r)T_j^{n} + rT_{j+1}^{n} \quad [4\text{-}12]$$

where T was temperature, the Fourier number $r = \alpha\ \Delta T/(\Delta X)^2$, $\Delta T = 900$ s was the time increment, and $\Delta X = 0.001$ m was the distance increment. The subscript j represented nodes in the space domain ranging from j=0 at the surface to j=300 at 30 cm. The superscript n represented nodes in the time domain ranging from n=0 to n=N where N represented the number of time increments in the problem. Equation 4-12 represents the Crank-Nicolson modified implicit method which is stable for all values of the Fourier number, and which has a truncation error of the order of $(\Delta T)^2 + (\Delta X)^2$ (Ozisik 1980, p. 493).

The boundary conditions were, in finite difference form,

$$T_0^n = f_0(n) \quad [4\text{-}13]$$

for j=0, and

$$T_{300}^n = f_{30}(n) \quad [4\text{-}14]$$

for j=300. For j=1 using Equation 4-13 in Equation 4-12 gives:

$$(2 + 2r)T_1^{n+1} - rT_2^{n+1} =$$
$$(2 - 2r)T_1^{n} + rT_2^{n} + rf_1(n) + rf_1(n+1) \qquad [4\text{-}15]$$

For j=300=N using Equation 4-14 in Equation 4-12 results in

$$-rT_{N-2}^{n+1} + (2 + 2r)T_{N-1}^{n+1} =$$
$$rT_{N-2}^{n} + (2 + 2r)T_{N-1}^{n} + rf_{30}(n) + rf_{30}(n+1) \qquad [4\text{-}16]$$

Equations 4-12, 4-15 and 4-16, when written out in matrix form for the N-1 interior nodes, result in two tridiagonal matrices each multiplied by an n by 1 vector. This system of equations is easily solved with a Thomas algorithm (See Appendix D for computer code). The initial condition was provided by setting the temperatures at the top and bottom nodes to their initial measured temperatures and setting the temperature at each node in the space domain to a value that varied linearly with distance between the surface and the bottom. This procedure introduced an initial distortion in heat flux which, however, degenerated to an insignificant value after one day of iteration time. When used for modeling purposes, the program was started using data that preceeded by one day the starting time for which calculations were desired.

The computer program was validated by setting the surface temperatures equal to a sine function of time:

$$T(0,t) = \overline{T} + A_0 \sin(2\pi t/24 + \phi_{0n}) \qquad [4\text{-}17]$$

where $\overline{T}$ is the average daily temperature, A_0 is the amplitude, ϕ_{0n} is the phase angle, and t is in hours; and letting the lower boundary equal the average temperature. For these boundary conditions a solution of Equation 4-1 is:

$$T(x,t) = \overline{T} + A_0 \exp(-x/D) \sin(wt - x/D) \qquad [4\text{-}18]$$

where $D = (2\alpha/w)^{1/2}$ (Monteith 1973 or Hillel 1982, Eq. 9.25). Taking the derivative of Equation 4-18 with respect to x, setting x to zero and using the result to replace $\partial T/\partial x$ in Equation 4-2 results in an equation predicting heat flux at the soil surface:

$$G = [kA_0(\sqrt{2})/D] \sin(wt + \pi/4) \qquad [4\text{-}19]$$

Integrating Equation 4-19 from $wt = -\pi/4$ to $3\pi/4$ gives the sum of diurnal positive heat flux which is:

$$G_{sum} = (\sqrt{2}) C_v A_0 D \qquad [4\text{-}20]$$

For given values of k and α the soil heat flux was calculated using the finite difference code and Equation 4-20, the results matching within 0.1% for the second, and subsequent, 24 hour periods of simulation. The net heat flux was 0.005 mm for the second and subsequent 24 hour periods versus zero for the analytical solution. These two results were considered to validate the computer code.

Soil heat flux, calculated by the finite differencing and using the sine wave function for surface temperature, is compared to that calculated using actual surface temperatures in Figure 4-5. Solar and net radiation are included for comparison. For this plot the phase angle in Equation 4-17 was set to -6 h which meant that soil surface temperature would rise above the average at 6 AM. As predicted by Equation 4-9, the start of positive soil heat flux preceeded that time by $\pi/4$ radians or 3 hours. Notably, the soil heat flux, calculated on the basis of actual temperatures, did not become positive until about 6:30 AM, about 1/2 hour after solar radiation became positive. For all days the soil heat flux based on actual temperatures became positive between 6:30 AM and 7:30 AM, just after sunrise. It became negative between 4:15 and 4:45 PM, about 3 hours before sunset. Thus it is clear that actual soil heat fluxes exhibit more complex behavior than predicted by the sine wave models of Equations 4-17 and 4-9. In particular the expected phase difference, between soil surface temperature (which is closely linked to solar radiation, see Figure 3-8) and soil heat flux, is practically non-existant at dawn but appears to be fully developed by sunset.

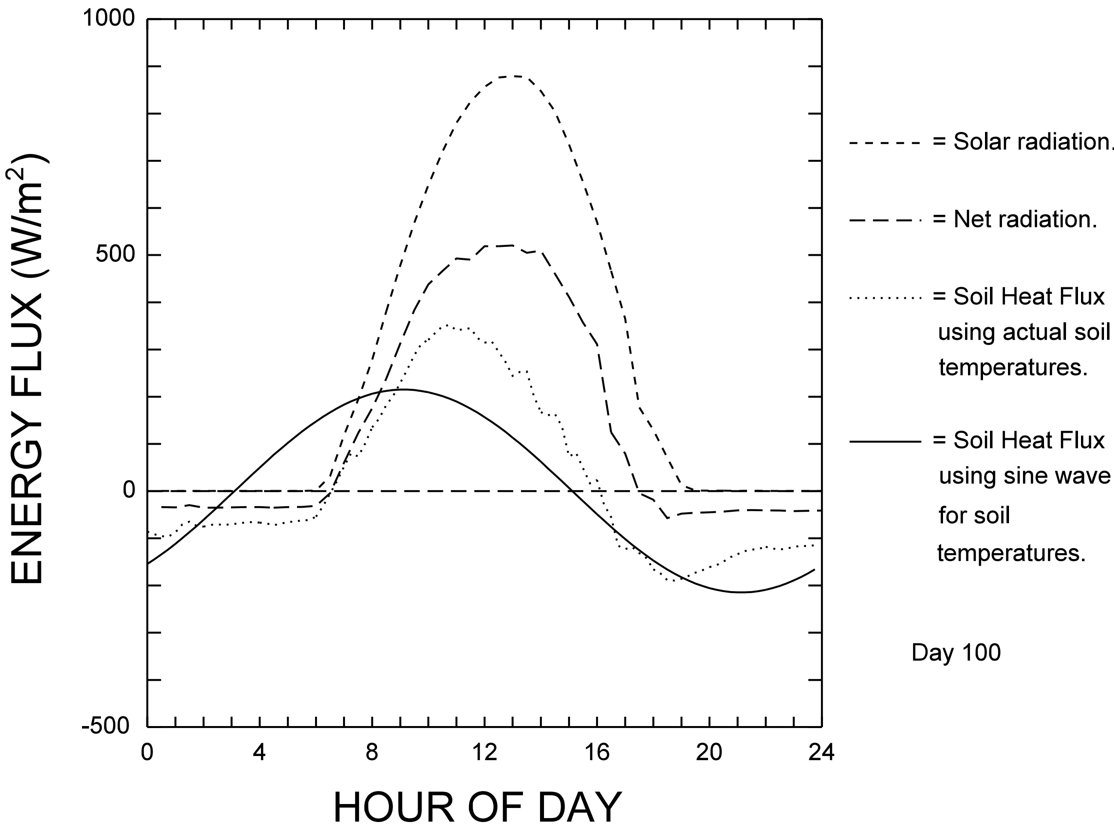

Figure 4-5. Comparison of soil heat flux calculated using actual soil temperatures to that calculated using temperatures from Equation 4-17. $\overline{T}$ = 34 and A_0 = 18 °C, and ϕ_{0n} = -6 h. Actual average temperature and amplitude were the same.

Calculation of daily net soil heat flux in the field soil involved using the surface and 30 cm measured temperatures, the diffusivities calculated with the harmonic method (for the 0 to 30 cm depth), the average daily soil water contents for 30 cm ML's, and heat capacity calculated by Equation 4-4. Net flux varied from 0.26 mm on the day after irrigation (when most solar radiation was converted to latent heat flux) to a high of 0.84 mm on the 6th day after irrigation with an average value of 0.67 mm (Figure 4-5, Table 4-11).

Table 4-11.

Positive (G) and net (net G) soil heat flux (mm of water equivalent) from implicit finite difference program IMPLIC2.BAS.

Code*	Day of Year 92	93	94	95	96	97	98	99	100	Averages
Field soil:										
G	2.41	2.63	2.73	2.91	2.86	3.03	2.47	2.85	2.79	2.78
net G	0.26	0.60	0.65	0.63	0.59	0.84	0.76	0.72	0.59	0.67
G - 1/2 net G	2.28	2.33	2.40	2.60	2.56	2.61	2.09	2.49	2.50	2.45
Microlysimeters:										
SC, net G	1.05	0.80	0.91	1.00	0.93	1.25	1.10	1.10	0.93	1.00
SO, net G	0.76	0.69	0.81	0.88	0.81	1.08	0.94	0.98	0.84	0.88
PC, net G	0.55	0.48	0.54	0.61	0.57	0.84	0.74	0.70	0.58	0.63
PO, net G	0.56	0.57	0.59	0.63	0.59	0.84	0.72	0.71	0.60	0.66
Average ML net G	0.73	0.64	0.71	0.78	0.73	1.00	0.88	0.87	0.74	0.79
Average closed ML net G	0.80	0.64	0.73	0.81	0.75	1.06	0.92	0.90	0.76	0.82

* Codes:
SC = steel ML with closed bottom.
SO = steel ML with open bottom.
PC = plastic ML with closed bottom.
PO = plastic ML with open bottom.
15 = surface to 15 cm layer.
30 = surface to 30 cm layer.

Since, over 24 hours, the sum of positive heat flux must exceed the sum of negative flux by the magnitude of the net flux, the positive heat flux minus 1/2 of the net heat flux was also plotted in Figure 4-4 to see how closely that quantity would match the positive heat flux calculated using the harmonic solution. The match was close, with the daily sum, of positive minus 1/2 net heat flux from finite differencing, averaging only 5% less than the positive heat flux from the harmonic solution.

Net heat fluxes calculated for both open and closed bottomed plastic ML's were very similar (Table 4-11, Figure

4-6). This is consistent with the fact that the average daily soil temperatures at 30 cm increased in much the same way for plastic ML's and the field soil (Figure 3-11). Since steel ML's showed a slightly more rapid increase in temperature at 30 cm it is also likely that net soil heat flux was larger in those ML's. Indeed, the calculated net flux for steel ML's averaged 44% higher than that of plastic ML's. Since net fluxes for plastic ML's and field soil were so similar, the field soil values will be used later for the purpose of investigating the validity of the first assumption in the energy balance model.

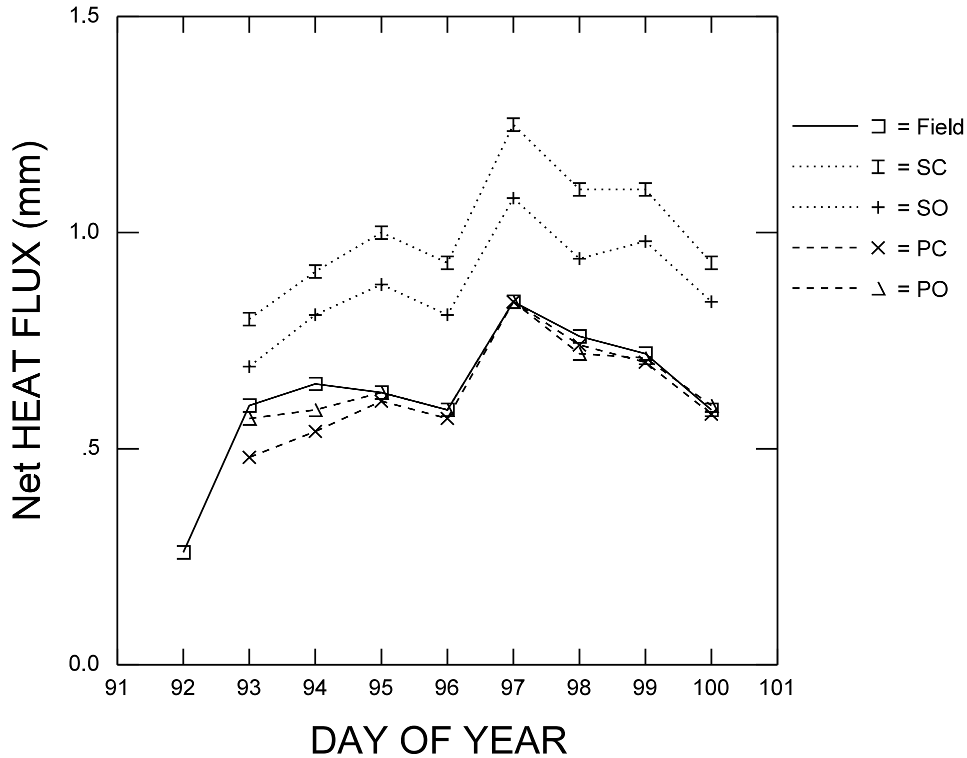

Figure 4-6. Net soil heat flux for field soil and microlysimeter treatments. Calculated for surface to 30 cm layer using finite difference program IMPLIC2.BAS and diffusivities from harmonic analysis. S = steel, P = plastic, O = open, and C = closed bottom.

<u>Summary</u>.

The data and analyses lead to the conclusion that wall material and length both affect the temperature regime of ML's in the field. Clearly the shorter ML's underestimated evaporation on later days since the closed bottoms prohibited the upward flow of soil moisture. Wall material caused important differences in evaporation measured for 20 and 30 cm long ML's and these differences were significant at the 10%

level for the 20 cm length. Steel ML's caused increased conduction of heat from the soil surface downward resulting in higher subsurface soil maximum temperatures. This may have resulted in increased nighttime vapor transport towards the surface due to warming of the lower soil. Field evidence for this increased vapor transport in steel ML's was observed in the early mornings for several days after irrigation when the soil surfaces were noticeably wetter (darker) in the steel ML's than in either the adjacent field or in the plastic ML's (Figure 4-7). Since the wetting caused lower soil albedo in the steel ML's the increased soil heat flux was partially balanced for short periods of time in the mornings by a decrease in reflected short wave radiation. It is possible that ML's in general over-estimated evaporation in the first few days after irrigation since capping the ML bottoms stopped drainage which left the soil inside wetter than adjacent field soil.

Figure 4-7. Photograph showing the difference in soil albedo between steel (darker) and plastic (lighter) ML's.